Applied Catalysis B: Environmental 160–161 (2014) 525–533

Contents lists available at ScienceDirect

Applied Catalysis B: Environmental

journal homepage: www.elsevier.com/locate/apcatb

Steam reforming of sulfur-containing dodecane on a Rh–Pt catalyst: Influence of process parameters on catalyst stability and coke structure

Qinghe Zheng[a], Christiane Janke[a,b], Robert Farrauto[a,*]

[a] Earth and Environmental Engineering Department, Columbia University, 500 West 120th Street, New York, NY 10027, United States
[b] BASF SE, GCC/PG – M301, Ludwigshafen 67056, Germany

ARTICLE INFO

Article history:
Received 26 February 2014
Received in revised form 21 May 2014
Accepted 23 May 2014
Available online 2 June 2014

Keywords:
Steam reforming
Sulfur-containing *n*-Dodecane
Rh–Pt catalyst
Preemptive regeneration
Process parameters

ABSTRACT

The present work offers a practical solution to the steam reforming (SR) of sulfur-containing liquid fuels, with dodecane as model compound for diesel fuel. The SR reaction is catalyzed by a Rh–Pt catalyst supported on a sulfur tolerant carrier (SiO_2–ZrO_2). The study highlights the influences of various process parameters such as steam to carbon (S/C) ratio, sulfur concentration, time on stream (TOS), and preemptive air regeneration on the catalytic performance and the nature of the deposited coke.

Stable catalytic performance of sulfur-free dodecane was achieved with S/C ratio >1.8. Catalyst deactivation was accelerated by the addition of increased amount of sulfur from 29 to 74 ppm. The formation of graphitic carbonaceous species was observed on the spent catalyst for higher sulfur concentrations and/or longer TOS. Preemptive air regeneration allowed more sustained catalytic activity under less severe conditions than conventional air regeneration. Moreover, the frequency of air regeneration had a profound effect on the nature of the coke formed. The study provides a possible economic and energy efficient solution to the industrial production of H_2 from sulfur-containing fuels.

1. Introduction

Hydrogen is well known as an alternative energy source with a high energy content. Proton-exchange membrane (PEM) fuel cell technology, with H_2 as a fuel, is an environmental friendly approach for generating both electricity and heat, with H_2O as the only byproduct [1–4]. Liquid fuels, such as methanol, ethanol, gasoline, and diesel can be converted to fuel-cell quality H_2 by reforming [5–8], followed by water gas shift reactions and CO preferential oxidation. Sulfur removal prior to reforming is always necessary for achieving sustained reforming activity [9,10], and is traditionally processed by hydrotreating or adsorption, which are both energy consuming processes. The current study is designed to reform heavy hydrocarbon fuels without sulfur removal. Among various reforming technologies for industrial production of hydrogen, SR is most appropriate for fuel cell applications for its enhanced hydrogen concentration in the crude reformate gas [11,12].

Diesel, with its existing logistic infrastructure, considerable well-to-wheel efficiency, safe handling feature, adequate world-wide fuel storage, and high energy density, is an attractive source of H_2 production via SR [13,14]. Diesel fuel is a complex mixture of hydrocarbon molecules with carbon numbers from 12 to 20. Compounds in diesel are categorized as alkanes, cycloalkanes, and aromatics. Sulfur is naturally present in diesel fuel as alkylbenzothiophene and alkyldibenzothiophene forms [15,16], and ultralow sulfur diesel (ULSD) with sulfur concentration below 15 ppm is now commercially available in United States and elsewhere. In the present work, *n*-dodecane ($C_{12}H_{26}$) was used as a model compound for diesel fuel, especially for its alkane fraction. High (74 ppm) and low (29 ppm) amounts of thiophene were added to the dodecane feed as surrogates for the organic sulfur in diesel fuel. The highly endothermic SR of *n*-dodecane reaction is expressed as Rx. (1) [17].

$$C_{12}H_{26} + 12H_2O \rightarrow 25H_2 + 12CO \quad \Delta H_{298\,K}{}^0 = 1866.5\,kJ/mol \qquad (Rx.\ 1)$$

Rhodium is known to be more active, and coke and sulfur tolerant than commonly used base metal catalysts such as Ni [18,19]. High intrinsic activity (activity/gram of catalyst) makes Rh containing SR catalysts suitable for deposition on heat exchangers for

* Corresponding author. Tel.: +1 732 829 7127; fax: +1 732 438 1090.
E-mail address: rf2182@columbia.edu (R. Farrauto).

http://dx.doi.org/10.1016/j.apcatb.2014.05.044
0926-3373/

compact reactor designs with enhanced heat transfer [20]. The catalyst carrier, which plays another significant role in SR, should not favor dehydrogenation reactions that produce olefins, which further promote coking. SiO_2 possesses low acidity, high surface area, reasonable thermal stability and sulfur tolerance, and hence is suitable for high temperature reactions [21–24]. ZrO_2 is another popular catalyst carrier with its stable surface area, and remarkably lower acidity compared to widely used Al_2O_3 [25]. Furthermore, ZrO_2 facilitates the adsorption of steam onto the support and the subsequent spillover of steam from the support to the active sites [26]. A Rh–Pt catalyst supported on SiO_2–ZrO_2 was therefore used in our study.

Catalyst deactivation still remains a major challenge in the processing of sulfur-containing heavy hydrocarbons [27,28]. Coking and sulfur poisoning commonly deactivate catalysts by selectively or non-selectively poisoning the active sites [29–32]. High reaction temperatures, low S/C, and the complex nature of sulfur-containing commercial diesel make coking especially favorable [33]. Olefins, typically ethylene, and aromatics are well known carbon-precursors, hence their formation must be reduced during the SR [34–37]. Additionally, catalysts with lower acidity were reported to be less prone to coking by suppressing dehydrogenation reactions [38,39]. H_2S, the main product in the reforming of organic sulfur, can bind to all transition metal catalysts to form metal–sulfur bonds and subsequently reduce catalyst activity by inhibiting the chemisorption of reforming reactants [40–42]. Meanwhile, the adsorbed sulfur species increases the catalyst acidity, and hence indirectly promotes coking [43,44]. Precious metal catalysts such as Rh and Pt have lower tendencies to form bulk sulfides than other metal catalysts such as Ni. Rh and Pt are less prone to sulfur poisoning by only chemisorbing sulfur rather than forming metal sulfides [45]. Farrauto et al. [20] have reported that the SR activity of methane using a Rh–Pt based catalyst could be completely recovered to its initial activity after the removal of sulfur from the feed stream, demonstrating the reversibility of sulfur adsorption on these metals.

The goal of this study is to investigate a practical solution for the industrial production of hydrogen by SR of sulfur-containing liquid fuel on a Rh–Pt/SiO_2–ZrO_2 catalyst, by controlling process variables including S/C ratio, time on stream (TOS), sulfur concentration, and preemptive air regeneration.

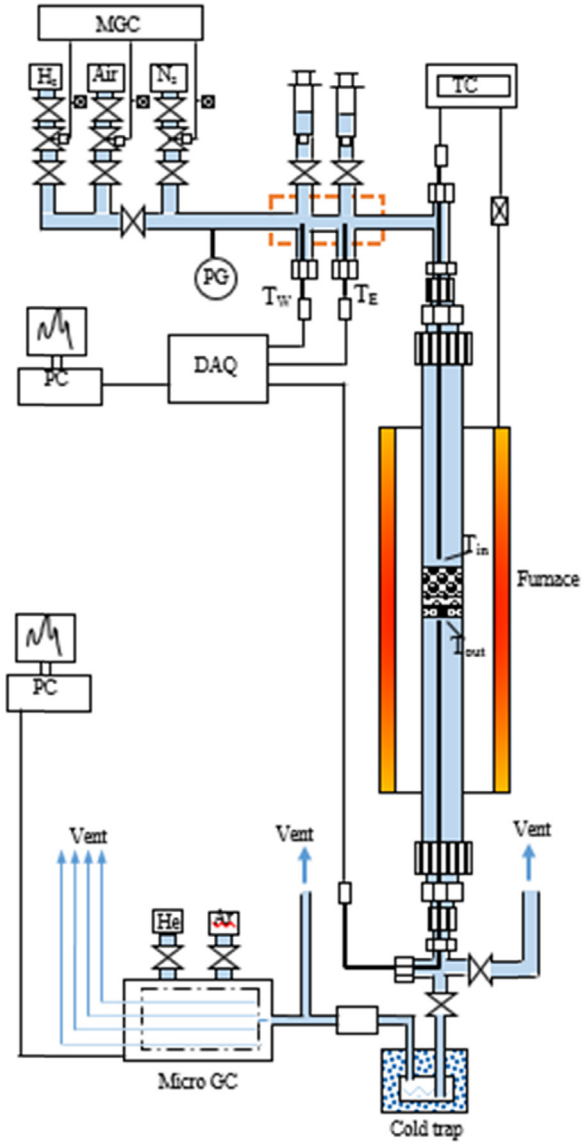

Fig. 1. Schematic of the reaction setup (MGC, multi gas controller; DAQ, data acquisition modules; PG, pressure gauge; TC, temperature process controller).

2. Experimental methodology

2.1. Catalyst and solution preparations

The ZrO_2–SiO_2 supported Rh–Pt catalyst was supplied by BASF. The precious metal loading was 4 wt% with Rh:Pt weight ratio of 3:1. The catalyst precursor salts and supports were proprietary BASF formulas. After impregnation, a 25% solid slurry was prepared, ball milled, and calcined. The initial dispersion of precious metal on the catalyst support was 22% as determined by CO chemisorption assuming a stoichiometry of CO: PM = 1 [46]. *n*-Dodecane (Signal–Aldrich) was selected as model compound for diesel fuel. Thiophene (Signal–Aldrich) was added to dodecane as a surrogate of organic sulfur naturally present in commercial diesel fuel.

2.2. Reactor apparatus and experimental process

Catalytic SR of dodecane was performed in a fixed bed reactor with a GHSV of 40,910 h^{-1} at 690 °C and atmospheric pressure. The schematic of the reactor is sketched in Fig. 1. 0.3 mL of catalyst particles were pressed, tabulated, sieved to 600–710 μm in diameter, and diluted with 1 mL quartz particles with the same particle sizes. The catalyst mixture was loaded into a quartz tube reactor (ID of 10.5 mm, OD of 12.7 mm) with a quartz frit fused in the middle. The reactor was housed in an infrared furnace (HOSKINS). Liquid fuel and water were pumped separately and continuously into the heated reaction system with syringe pumps (Cole Parmer). The vaporized reactants then combined with the incoming N_2 (diluent and internal standard), and passed through the catalyst bed. The unreacted liquid fuel and water were condensed in a cold trap located downstream. The remainder of the gas products with low boiling points were identified and quantified online using a four-channel Micro GC (Agilent 3000), equipped with Molsiev (10 m × 0.32 mm), Plot Q (8 m × 0.32 mm), OV-1 (14 m × 0.15 mm) and HP-Innowax (10 m × 0.25 mm) columns, and thermal conductivity detectors. Each product sample was automatically injected into the micro-GC every 4 min. The inlet gas flow was controlled by Multi Gas Controller (MKS 647C) equipped with individual mass flow controllers. The heat for the reactor was supplied by an electric infrared furnace (HOSKINS FD303), while the heat for evaporators was supplied by flexible heating tapes (Omega FGS). The real-time temperature signals for the water evaporator (T_W, 250 °C), fuel evaporator (T_E, 250 °C), catalyst inlet (T_{in}), and outlet (T_{out}) were monitored online (Omega USB Data Acquisition Modules).

The transient reaction temperature T_r (around 690 °C) was taken by averaging T_{in} and T_{out}.

2.3. Catalytic tests

SR of pure dodecane with S/C ratios of 2.5, 1.8, and 1.6 (stoichiometric S/C = 1) were performed to explore the appropriate coke-free reaction conditions. High (74 ppm) and low (29 ppm) doses of sulfur were later added to the dodecane feed. The high concentration sulfur was used to accelerate catalyst deactivation, while the low concentration sulfur was selected to closely simulate the sulfur content in commercial diesel (<15 ppm). SR of sulfur-containing (74 ppm) dodecane tests were also performed with various TOSs (50 min, 100 min, and 200 min). SR cycle tests of high concentration (74 ppm) sulfur-containing dodecane with preemptive air regenerations, were subsequently performed with 200 min- and 100 min-TOS per cycle. In between each SR cycle, dodecane injection was suspended with air pumped in at a flow rate of 0.7 L/h. The regeneration was stopped once the CO_2 in the product stream was detected below 1 vol.%. The SR-preemptive regeneration cycle tests of low concentration (29 ppm) sulfur-containing dodecane was also studied.

2.4. Catalyst characterization

SEM measurements of the spent catalysts were conducted with HITACHI S-4700 I Cold Field Emission Scanning Electron Microscope. Accelerating voltage of 5 kV, emission current of 10 μA, working distance of 12 mm were chosen as the working conditions for the measurements. Multiple pictures were taken for each measured sample at different locations.

In order to estimate the amount of coke generated during SR, TPO measurements were carried out with the spent catalysts using ChemBET Pulsar TPR/TPD unit (Quantachrome). Each catalyst sample (about 0.05 g) was degassed in helium with a flow rate of 80 mL/min at 140 °C for 40 min. TPO was then performed by ramping temperature from 40 °C to 900 °C at 5 °C/min in 3% O_2/He at 15 mL/min. Water generated during the TPO measurements was condensed in a cold trap.

Raman Spectra of the fresh and spent catalyst samples were obtained by HORIBA LabRAM ARAMIS spectrometer equipped with OLYMPAS BX41 microscope (50× magnification) and a thermo-electrically cooled CCD detector, to analyze the chemical structure of surface carbon. The samples were excited with Yag DPSS laser at 532 nm, with spectra acquisition of 1 exposure time per second, 20 s of exposure time per accumulation, and 2 accumulations per measurement. Each sample was measured 5 times at different spots.

2.5. Data analysis

The mole flow Q_i (mol/h) of the following gas components in the product stream were determined by Eq. (1): H_2, O_2, N_2, CO, CH_4, CO_2, C_2H_4, C_2H_6, C_3H_6, and C_3H_8.

$$Q_i = Q_{N_2} \times \frac{F_i}{F_{N_2}} \quad (1)$$

where Q_{N_2} was the mole flow rate of the input N_2 (internal standard, 0.3247 mol/h). F_i was the mole fraction of gas product i in the product stream, which was quantified by the micro GC.

Unconverted liquid fuels and water were condensed before entering the micro GC. The gas phase products were quantified by an online GC, except coke, which was deposited on the catalyst surface and not measured. However, the amount of deposited carbon in each test was insignificant compared with that in the bulk gas products. Consequently, the conversions of the reactants could be calculated based on the mole amount of the material input and output.

The conversions of liquid fuel (dodecane/diesel) X_{fuel}, and water X_{water} were defined as:

$$X_{fuel} = \frac{\text{Total mole amount of C in gas reformate}}{\text{Total mole amount of C in } C_nH_m \text{ feed}} \times 100\% \quad (2)$$

$$X_{water} = \frac{\text{Total mole amount of O in gas reformate}}{\text{Total mole amount of O in } H_2O \text{ feed}} \times 100\% \quad (3)$$

(expressed as mole flows).

The mole amounts of output carbon and oxygen were calculated from the mole flows (Q_i) of detected components in the reformate gas. When input and product carbon were balanced, there should be no hydrocarbon species condensed in the cold trap, and hence the reformed fuel was completely converted $X_{fuel} = 100\%$. When the product carbon in the gas phase was less than the input, the reformed fuel was not fully converted ($X_{fuel} < 100\%$), indicating deactivation of the catalyst. The fuel/water conversion was calculated as the difference between carbon/oxygen input and output gas phase carbon/oxygen. The source of oxygen is from H_2O. Thermodynamic equilibrium calculations were simulated by *HSC Chemistry 5* Program.

3. Results and discussion

3.1. SR of pure n-dodecane with various S/C ratios

High steam to carbon (S/C) ratios favor high conversions and H_2 production, with reduced coking [47–51]. Although the catalytic performance can be improved by increasing S/C, an energy penalty is accompanied due to heat consumption in steam vaporization. Consequently, S/C ratio should be minimized for energy efficiency. We have calculated that an additional 549 kJ/h is required for a S/C of 2.5 vs. 1.8 (used in our study) when processing every mol/h of dodecane. The energy expended for pre-emptive regeneration is only 140 kJ/h. Furthermore the elimination of the HDS process provides a major economic savings.

Fig. 2 depicts the conversion profiles of reactants and products in the SR of pure *n*-dodecane with S/C of 2.5, 1.8, and 1.6 (with stoichiometric S/C of 1.0). Equilibrium conversions were reached for all tests. With S/C ≥1.8, catalytic activity was sustained for as long as 800 min. On the contrary, significant catalyst deactivation was observed with S/C of 1.6, with the conversions of dodecane and water decreasing by 22% and 26% respectively after a total 650 min TOS. Catalyst deactivation coincided with the increased productions of ethylene and ethane (Fig. 3). The production of ethylene, which is a coke precursor, was promoted by reducing S/C, especially from 1.8 to 1.6. Higher S/C specifically S/C ≥1.8 enhances the catalyst stability, and presumably minimizes carbonization reactions. To maximize catalytic performance and minimize energy consumption at the same time, S/C of 1.8 was chosen as the reaction condition for further study.

3.2. SR of n-dodecane with different sulfur concentrations

Immediate catalyst deactivation was observed with the addition of sulfur to the dodecane feed (Fig. 4). With 29 ppm sulfur present, reductions of 20% and 17% were observed for dodecane and water conversions after a total 200 min-TOS, compared to higher reductions of 31% and 59% when an accelerated aging test was performed with 74 ppm sulfur. The productions of H_2, CO, CO_2 and CH_4 maintained equilibrium for the sulfur free feed but were not sustained with sulfur present. A reduction of 37% in H_2 production

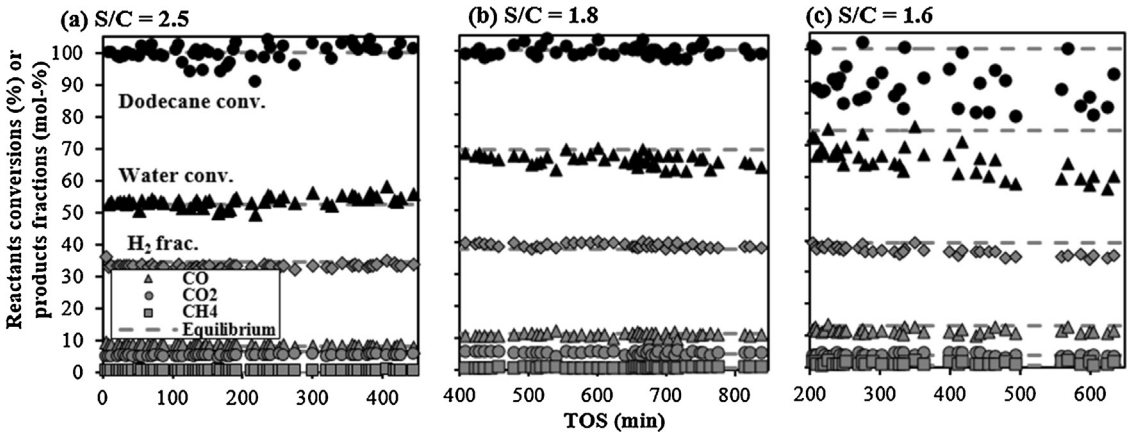

Fig. 2. Conversions of dodecane and water, and mole fractions of main products (H_2, CO, CO_2, CH_4) as a function of TOS with different S/C ratios for the catalytic SR of pure *n*-dodecane, with stoichiometric S/C of 1.0. (a) S/C = 2.5, (b) S/C = 1.8, and (c) S/C = 1.6. GHSV = 40,910 h^{-1}, at 690 °C and 1 atm.

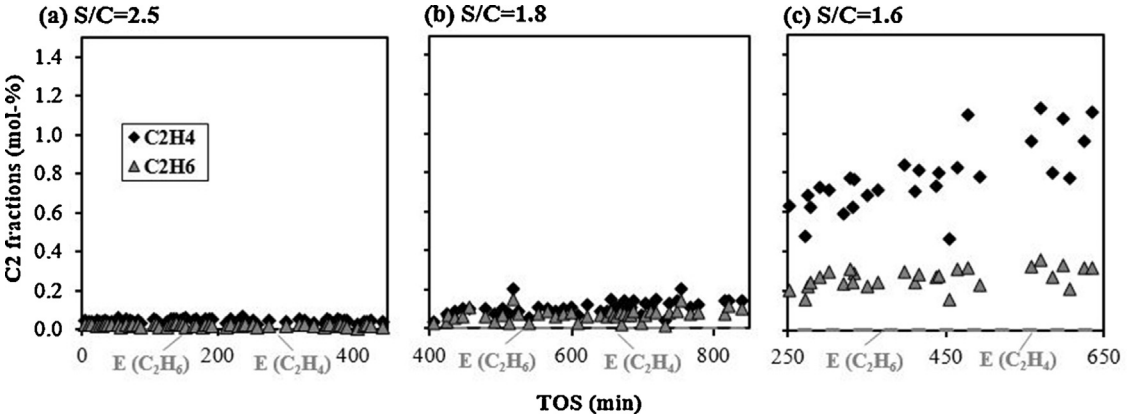

Fig. 3. Mole fractions of coke precursors (C_2H_4, and C_2H_6) as a function of TOS with different S/C ratios for the catalytic SR of pure *n*-dodecane, with stoichiometric S/C ratio of 1.0. (a) S/C = 2.5, (b) S/C = 1.8, and (c) S/C = 1.6. GHSV = 40,910 h^{-1}, at 690 °C and 1 atm.

was observed for the 74 ppm sulfur feed compared to a reduction of only 14% for 29 ppm sulfur feed. Meanwhile, the formations of ethylene and ethane continuously increased with increasing sulfur concentration (Fig. 5). Carbonaceous side reactions were expected to occur when high concentration of sulfur was present in the feed stream.

The SEM images of spent catalysts after SR of dodecane with 74 ppm and 29 ppm sulfur (Fig. 6) revealed the formation of carbonaceous species. Coking was favored in the presence of higher concentration of sulfur, with larger sizes of carbonaceous particles observed. The average size of carbon particles deposited on spent catalysts after SR of 74 ppm sulfur-containing dodecane was almost

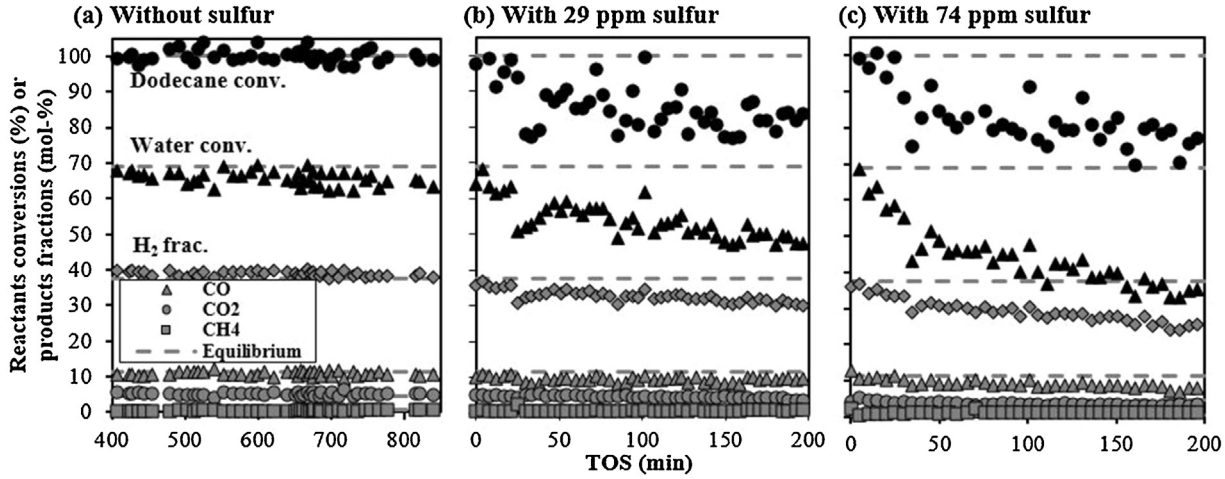

Fig. 4. Conversions of dodecane and water, and mole fractions of main products (H_2, CO, CO_2, CH_4) as a function of TOS for SR of *n*-dodecane (a) without sulfur, (b) with 29 ppm sulfur, and (c) with 74 ppm sulfur in dodecane feed. GHSV = 40,910 h^{-1}, S/C = 1.8, at 690 °C and 1 atm.

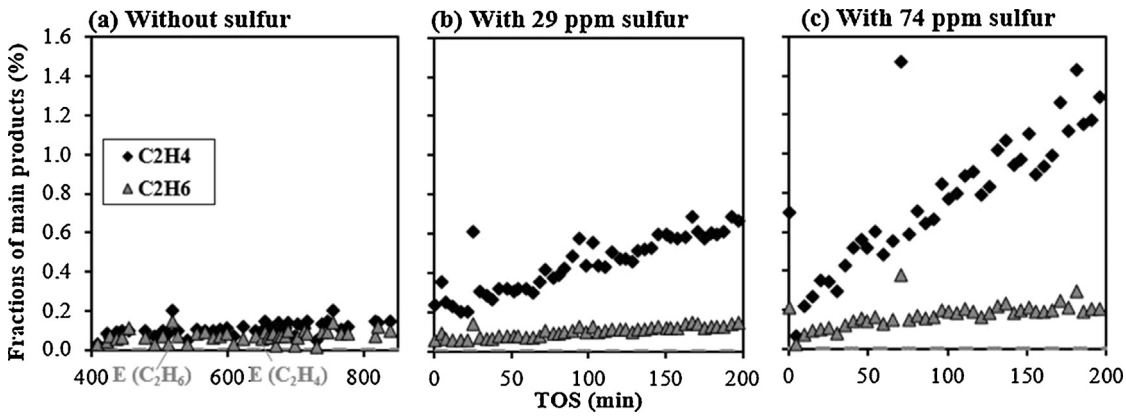

Fig. 5. Mole fractions of coke precursors (C_2H_4 and C_2H_6) as a function of TOS for SR of *n*-dodecane (a) without sulfur, (b) with 29 ppm sulfur, and (c) with 74 ppm sulfur in dodecane feed. GHSV = 40,910 h^{-1}, S/C = 1.8, at 690 °C and 1 atm.

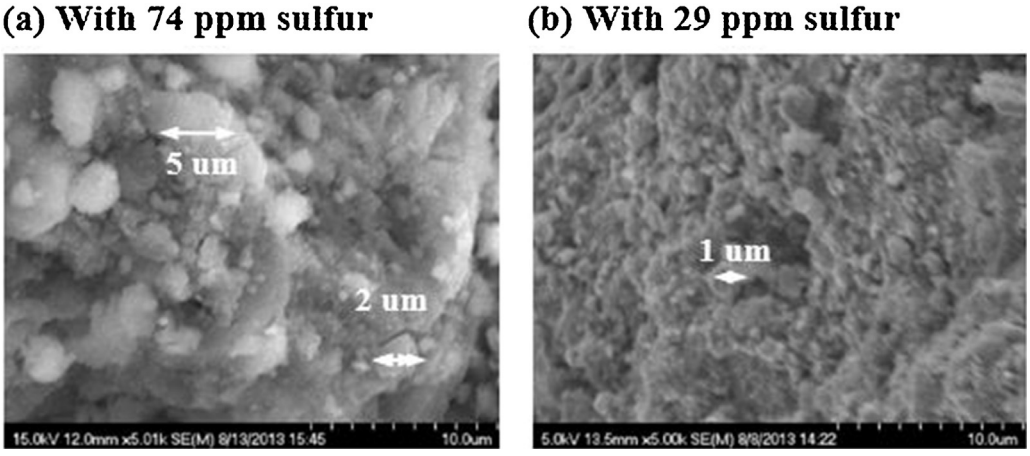

Fig. 6. SEM images of spent catalysts after SR of *n*-dodecane with different sulfur concentrations: (a) with 74 ppm sulfur after 200 min-TOS, and (b) with 29 ppm sulfur after 360 min-TOS.

twice as that of the same feed but with 29 ppm, even though longer TOS was applied on the latter.

TPO measurements were performed to quantify the amount of surface carbon generated on the spent catalysts. The amount of CO_2 produced during TPO was detected every 90 seconds by an online micro GC, and was plotted as a function of TOS (Fig. 7). Two predominant carbon peaks within the temperature ranges of 485–545 °C and 565–709 °C, annotated as P_1 and P_2, were generated. The peak intensity is proportional to the carbon amount, while the peak position reflects the coke nature. More refractory and higher amount of coke was formed on spent catalysts after processing 74 ppm sulfur containing dodecane, in agreement with the SEM observations.

Raman spectra (Fig. 8) shows the well-defined D band (around 1340 cm^{-1} wavenumber) and G band (around 1590 cm^{-1} wavenumber) for the carbon deposited on spent catalysts after SR of 29 or 74 ppm sulfur-containing dodecane. D band is

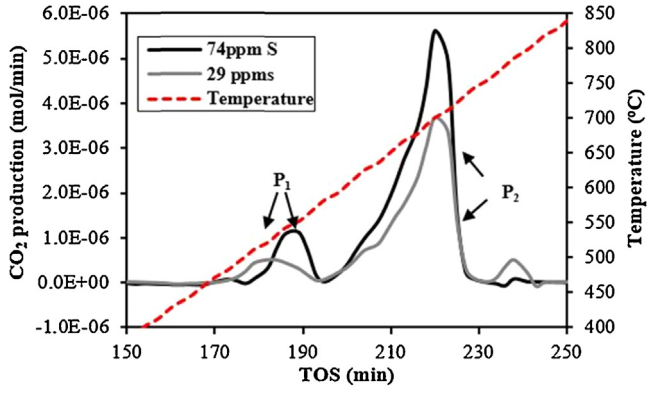

Fig. 7. CO_2 mole production with increasing temperature as a function of TOS in the TPO measurements of spent catalysts after SR of *n*-dodecane with different sulfur concentrations. Solid line: with 74 ppm sulfur after 200 min-TOS; Dashed line: with 29 ppm sulfur after 360 min-TOS.

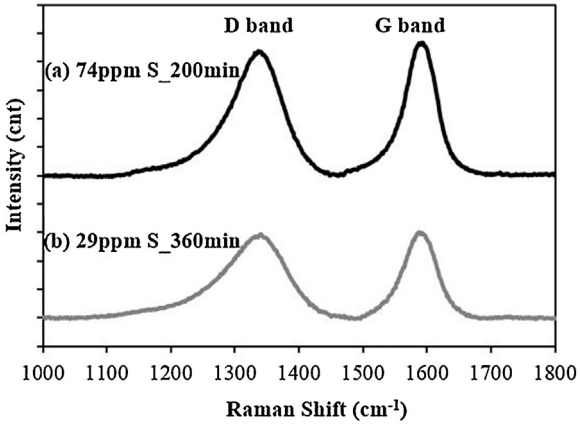

Fig. 8. Raman spectra of spent catalysts after SR of *n*-dodecane with different sulfur concentrations. (a) with 74 ppm sulfur after 200 min-TOS, and (b) with 29 ppm sulfur after 360 min-TOS.

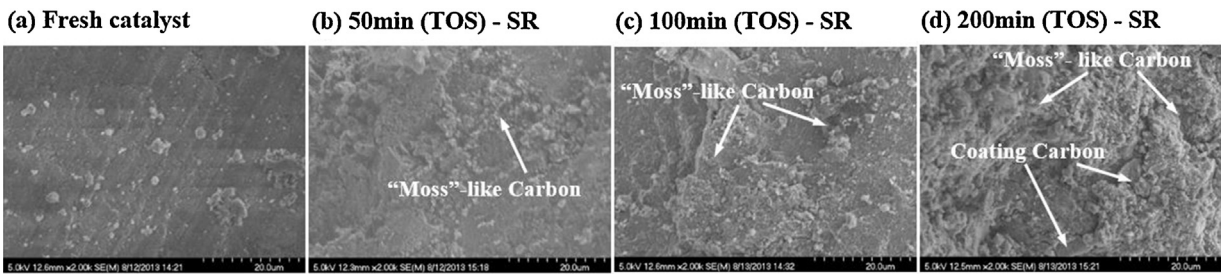

Fig. 9. SEM images of fresh or spent catalysts after different TOS of SR of *n*-dodecane (with 74 ppm sulfur) tests. (a) for fresh catalyst; (b), (c), (d) for spent catalysts after 50 min, 100 min and 200 min TOS, respectively.

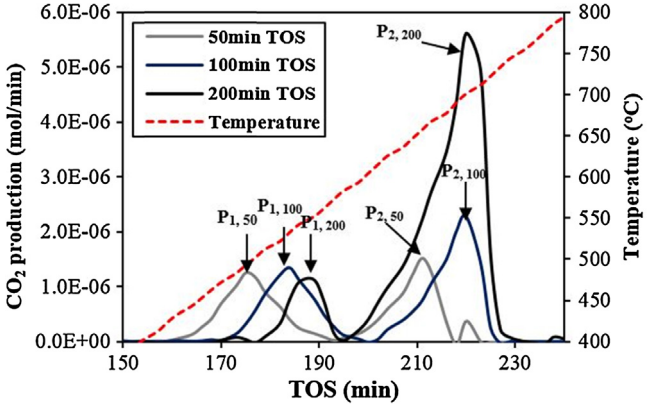

Fig. 10. CO_2 mole production with increasing temperature as a function of TOS in the TPO measurements of spent catalysts after 50 min, 100 min, and 200 min-TOS SR tests with 74 ppm sulfur present.

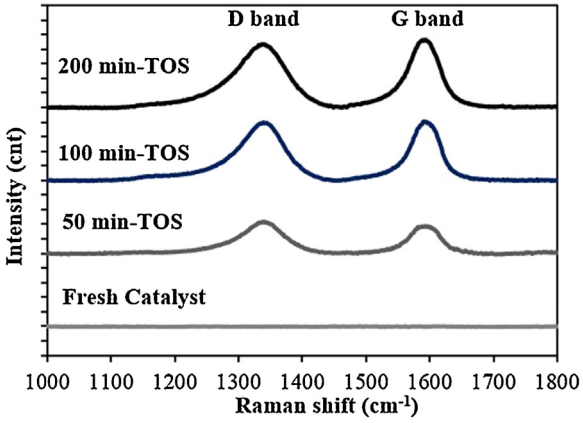

Fig. 11. Raman spectras of spent catalysts after 50 min-, 100 min-, and 200 min-TOS SR with 74 ppm sulfur, in comparison with the fresh catalyst.

Table 1
Raman spectroscopic parameters of carbonaceous species deposited on spent catalysts after SR of 29 or 74 ppm sulfur-containg dodecane.

Spent catalysts	Raman shift (cm^{-1})		I_G/I_D	L_a (mm)
	D-band	G-band		
SR of dodecane (29 ppm-S, 360 min TOS)	1340	1589	1.02	4.49
SR of dodecane (74 ppm-S, 200 min TOS)	1336	1592	1.07	4.71

Table 2
Raman spectroscopic parameters of carbonaceous species deposited on spent catalysts after SR of dodecane (74 ppm) with different TOS.

Spent catalysts	Raman shift (cm^{-1})		I_G/I_D	L_a (mm)
	D-band	*G*-band		
SR of dodecane (74 ppm-S, 200 min TOS)	1336	1592	1.07	4.71
SR of dodecane (74 ppm-S, 100 min TOS)	1339	1590	1.02	4.49
SR of dodecane (74 ppm-S, 50 min TOS)	1338	1593	0.86	3.78

ascribed to poorly structured carbon deposits with C–H deformation (amorphous carbon), while G band is related to in-plane sp^2 carbon–carbon stretching vibrations of well-structured coke or graphite-like structures. Furthermore, the average crystal diameter L_a can be calculated using Tuinstra–Koenig's law: $L_a(\text{nm}) = 4.4(I_G/I_D)$, where I_G and I_D are intensities of G and D bands [52]. Larger L_a indicates a higher ordering (graphitization) degree of carbonaceous species [53–56]. L_as for spent catalysts after SR of 29 ppm or 74 ppm sulfur-containing dodecane are listed in Table 1. The graphitization degree of carbon deposited on the spent catalyst surface increases with increasing sulfur concentration. Graphitic coke is more difficult to be removed during regeneration and can therefore significantly impact the catalyst life.

In summary, catalyst deactivation is enhanced with increasing sulfur concentration in the feed. Sulfur poisoning, accompanying enhanced coke formation, is suspected to be the major mechanism for catalyst deactivation. Increased catalyst acidity, due to sulfur adsorption on the precious metals, can indirectly induce deactivation by promoting graphitic coking via ethylene formation. The increased amounts of carbonaceous and sulfur may negatively impact SR by reducing total catalytic surface area and changing coke morphology.

3.3. SR of n-dodecane (with 74 ppm sulfur) with different TOS: accelerated aging tests

Catalyst can be deactivated by the direct masking by coke. Fig. 9 showed the SEM images of spent catalysts after 50 min-, 100 min-, and 200 min-TOS of SR of dodecane (with 74 ppm sulfur). Coarser surfaces correspond to denser carbonaceous groups after longer TOS. Specifically, "moss"-like carbon with diameters less than 1 μm was found to be the dominant carbon morphology after 50 min- and 100 min-TOS, while large amounts of bulk crystallized carbon, with average diameters of 1–6 μm predominated on the surface after 200 min-TOS. With longer TOS, carbonaceous species form more complicated structures by dehydrogenation, further causing plugging of catalyst pores, and eventually resulting in the catalyst deactivation.

The TPO measurements of spent catalysts are depicted in Fig. 10. The amount of CO_2 produced during the TPO tests was plotted as a function of TOS. Similar as before, two predominant carbon peaks $P_{1,TOS}$ and $P_{2,TOS}$, corresponding to poorly structured carbon and refractory coke were generated. More refractory and higher amount of coke was formed on spent catalysts after longer

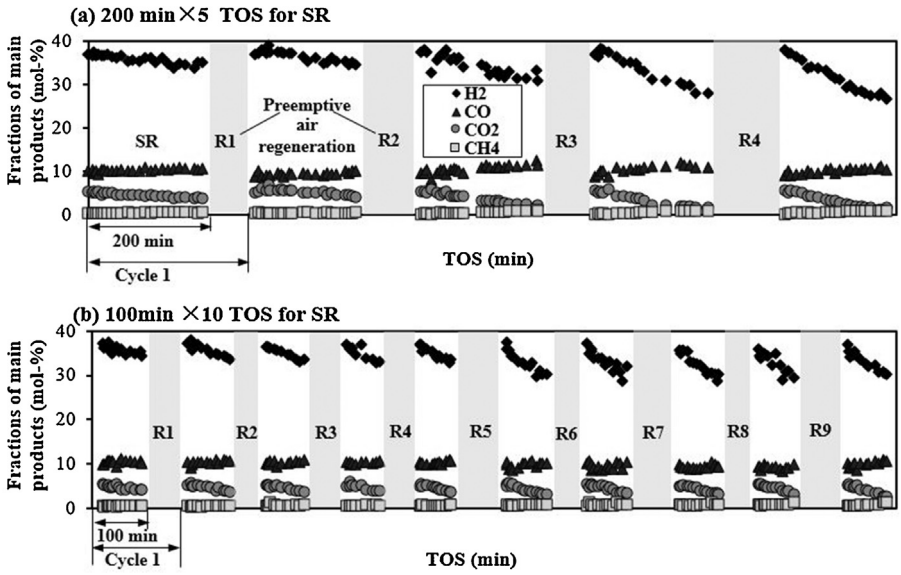

Fig. 12. Mole fractions of main products (H_2, CO, CO_2, and CH_4) as a function of TOS for SR-preemptive air regeneration of *n*-dodecane (with 74 ppm sulfur) with different regeneration frequencies. (a) 200 min-TOS and (b) 100 min-TOS for SR per cycle, total 1000 min for the SR process in both tests. GHSV = 40,910 h^{-1}, S/C = 1.8, at 690 °C and 1 atm.

TOS. Distinct differences of the peak intensities were observed at high temperatures, when the combustion of refractory coke dominated. Significantly higher amount of refractory coke was formed on the spent catalyst after longer TOS. Although the amount of poorly structured coke observed at lower temperatures did not vary much, the increased refractory nature was revealed by the high temperature-shifted P_1 with longer TOS.

Raman spectroscopic results of spent catalysts after different TOS of 74 ppm sulfur containing dodecane is shown in Fig. 11 and Table 2. The *D* band and *G* band, corresponding to amorphous and graphitic carbonaceous species, were generated for all of the spent catalysts, compared to the flat curve for fresh catalyst. L_a increases with TOS, indicating the increased ordering degree of surface carbon.

To summarize, amorphous and graphitic carbon were observed on all of the spent catalyst samples, and enhanced graphitic coking was observed with longer TOS. Graphitic carbon prevents effective regeneration due to its refractory nature, resulting in a shorter catalyst life. Sulfur accumulation on the catalyst surface with TOS, causing significant increase in surface acidity, enhances coking via ethylene formation, and is considered the main cause of graphitic coking. The continuous accumulation of carbon and sulfur enhance catalyst deactivation resulting in difficulties in effective regeneration.

3.4. SR-preemptive air regeneration

3.4.1. SR-preemptive air regeneration of n-dodecane with 74 ppm sulfur

In industrial process coke is regenerated after the catalyst has shown significant deactivation with TOS. In situ preemptive air regeneration is an effective approach to completely restore catalyst activity by removing deposited coke and sulfur from the catalyst surface. Unlike conventional air regeneration which were performed with longer TOS (15–40 h) of SR per cycle [57–60], preemptive air regeneration is a process conducted prior to any notable catalyst deactivation, and has been shown effective in the SR of E85 fuel [61]. More rapid catalyst deactivation and increasing difficulties in regeneration are the main issues associated with conventional air regeneration technology. Irreversible structural changes of the coke and catalyst account for the unrecovered activity.

Preemptive air regeneration was effective in postponing catalyst deactivation by removing the coke and adsorbed sulfur before graphitic carbon was formed. Fig. 12 profiles the production of the main products in the SR-preemptive air regeneration cycles of *n*-dodecane (with 74 ppm sulfur present) at 100 min-TOS. For both SR-preemptive regeneration cycles with different TOSs, initial catalytic performance was restored completely after

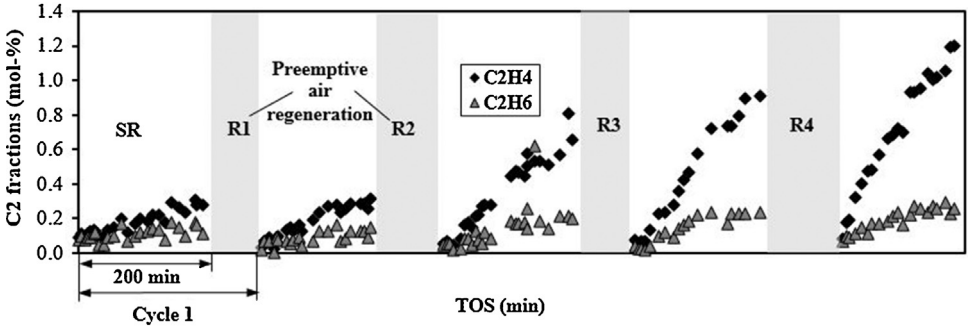

Fig. 13. Mole fractions of coke precursors (C_2H_4, and C_2H_6) as a function of TOS for SR-preemptive air regeneration of *n*-dodecane (with 74 ppm sulfur) with 200 min (TOS) for SR per cycle. GHSV = 40,910 h^{-1}, S/C = 1.8, at 690 °C and 1 atm.

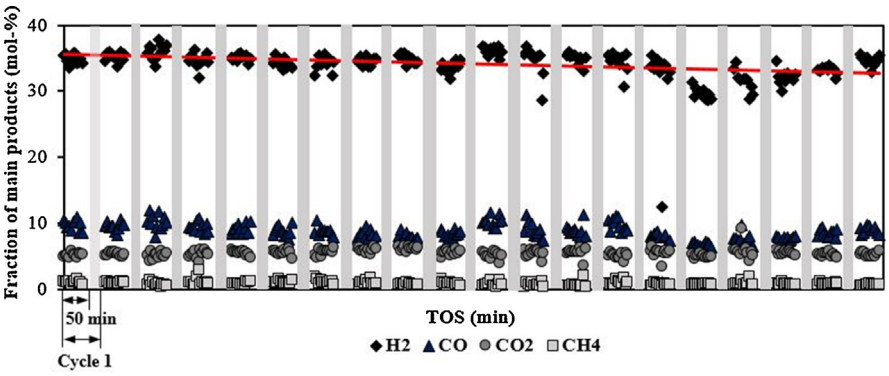

Fig. 14. Mole fractions of main products (H_2, CO, CO_2, and CH_4) as a function of TOS for SR (50 min, 20×) – preemptive air regeneration of *n*-dodecane with 29 ppm sulfur present, total 1000 min (TOS) for the SR process in both tests. GHSV = 40,910 h^{-1}, S/C = 1.8, at 690 °C and 1 atm.

regeneration. However, increased catalyst deactivation rates and C_2 productions were observed (Fig. 13) with longer TOS. Inevitably, refractory carbon was accumulated on the catalyst surface with longer TOS. Longer regenerations, indicating more difficult catalyst reactivation, were required for later cycles. Compared to 200 min (TOS), a lower catalyst deactivation rate was observed with 100 min SR (TOS) – regeneration cycles. The catalytic performance of SR and WGS reactions were more effectively sustained with frequent preemptive air regeneration probably by reducing the formation of graphitic carbon.

3.4.2. SR-preemptive air regeneration of n-dodecane with 29 ppm sulfur

Stable catalytic performance was observed in the SR (50 min TOS) – preemptive air regeneration cycle tests with 29 ppm sulfur present (Fig. 14). SR with frequent air regenerations provides a potential approach for achieving sustained catalytic activity when processing logistic diesel fuel. To improve the H_2 production efficiency, swing reactors are suggested to simultaneously perform SR reactions and catalyst regenerations.

4. Conclusions

Catalytic SR of sulfur containing-dodecane was performed with a Rh–Pt/ZrO_2–SiO_2 catalyst. Catalytic performance was controlled by engineering the process parameters including S/C ratio, sulfur concentration, TOS, and preemptive air regeneration. Influences of process parameters on catalyst stability and coke structure were studied.

Higher S/C ratios positively favor catalyst stability of the SR reaction of sulfur free dodecane, while simultaneously minimizing carbonization side reactions. Rapid catalyst deactivation was observed with S/C = 1.6, while relatively stable catalytic performance was achieved when S/C ≥1.8. To simultaneously sustain catalytic stability and minimize energy consumption, S/C = 1.8 was considered the appropriate condition for further studies.

Catalyst deactivation instantly occurred by the addition of sulfur compounds, and was further enhanced with increasing sulfur concentration (74 ppm rather than 29 ppm sulfur) in the feed stream. Coking, promoted by the increased sulfur concentration, appears to be another deactivation mechanism. When exposed to a higher concentration of sulfur, increased amounts and graphitization of carbonaceous particles form on the catalyst surface, changing the surface morphology of the coke to a more refractory nature.

Enhanced graphitic coking was experienced by catalysts with longer TOS. Sulfur accumulation on the catalyst surface, enhancing coke formation via ethylene formation, is considered the main cause of graphitic coking. Without controlled regeneration, graphitic coke forms readily.

Preemptive air regeneration was effective in restoring catalytic activity by removing coke and adsorbed sulfur from the catalyst surface before any notable catalyst deactivation occurs. More frequent preemptive air regenerations improved catalytic stability by removing the coke before carbon with graphitic carbon was formed. Stable catalytic performance was observed with preemptive air regeneration of *n*-dodecane with 29 ppm sulfur, providing the possibility of stable SR of commercial low sulfur-containing fuels.

To implement preemptive regeneration of sulfur-containing fuels one can envision swing reactors in parallel where one is reforming the feed while the other is being regenerated.

Acknowledgments

The authors would like to thank BASF for research support and supplying the catalyst. Meanwhile, the authors extend their gratitude to Dr. Ioannis Valsamakis, Zhuochang Yang, Dr. Amanda Simson and all other members of the Catalysis for a Sustainable Environment group in Columbia University.

References

[1] S. Ahmed, M. Krumpelt, Int. J. Hydrogen Energy 26 (2001) 291–301.
[2] A.F. Ghenciu, Curr. Opin. Solid State Mater. Sci. 6 (2002) 389–399.
[3] R.F. Mann, J.C. Amphlett, M.A.I. Hooper, H.M. Jensen, B.A. Peppley, P.R. Roberge, J. Power Sources 86 (2000) 173–180.
[4] T. Berning, D.M. Lu, N. Djilaili, J. Power Sources 106 (2002) 284–294.
[5] C.H. Bartholomew, R.J. Farrauto, Fundamentals of Industrial Catalytic Processes, second ed., John Wiley & Sons, Inc., New Jersey, 2006.
[6] S.H. Clarke, A.L. Dickes, K. Pointon, T.A. Smith, A. Swann, Catal. Today 38 (1997) 411–423.
[7] A. Ersoz, H. Olgun, S. Ozdogan, C. Gungor, F. Akgun, M. Tiris, J. Power Sources 118 (2003) 384–392.
[8] P.D.F. Vernon, M.L.H. Green, A.K. Cheetham, A.T. Ashcroft, Catal. Lett. 6 (1990) 181–186.
[9] T.V. Choudhary, D.W. Goodman, Catal. Today 77 (2002) 65–78.
[10] A. Cutillo, S. Specchia, M. Antonini, G. Saracco, V. Specchia, J. Power Sources 154 (2006) 379–385.
[11] Q. Ming, T. Healey, L. Allen, P. Irving, Catal. Today 77 (2002) 51–64.
[12] V.S. Guggilla, J. Akyurtlu, A. Akyurtlu, I. Blankon, Ind. Eng. Chem. Res. 49 (2010) 8164–8173.
[13] S. Haji, C. Erkey, Ind. Eng. Chem. Res. 42 (2003) 6933–6937.
[14] J. Boon, E. van Dijk, S. de Munck, R. van den Brink, J. Power Sources 196 (2011) 5928–5935.
[15] M.V. Mundschau, C.G. Burk, D.A. Gribble, Catal. Today 136 (2008) 190–205.
[16] M.C. Alvarez-Galvan, R.M. Navarro, F. Rosa, Y. Briceno, F. Gordillo Alvarez, J.L.G. Fierro, Int. J. Hydrogen Energy 33 (2008) 652–663.
[17] J. Zheng, J.J. Strohm, C. Song, Fuel Process. Technol. 89 (2008) 440–448.
[18] J. Sehested, Catal. Today 111 (2006) 103–110.
[19] R.K. Kaila, A. Gutierrez, S.T. Korhonen, A.O.I. Krause, Catal. Lett. 115 (2007) 70–78.
[20] R.J. Farrauto, Y. Liu, W. Ruettinger, O. Ilinich, L. Shore, T. Giroux, Cat. Rev. Sci. Eng. 49 (2007) 141–196.

[21] A.J. Vizcaino, A. Carrero, J.A. Calles, Int. J. Hydrogen Energy 32 (2007) 1450–1461.
[22] M.C. Ribeiro, G. Jacobs, B.H. Davis, L.V. Mattos, F.B. Noronha, Top. Catal. 56 (2013) 1634–1643.
[23] G. Agostini, R. Pellegrini, G. Leofanti, L. Bertinetti, S. Bertarinone, E. Groppo, A. Zecchina, C. Lamberti, J. Phys. Chem. 113 (2009) 10485–10492.
[24] A. Auroux, A. Gervasini, J. Phys. Chem. 94 (1990) 6371–6379.
[25] M.H. Youn, J.G. Seo, H. Lee, Y. Bang, J.S. Chung, I.K. Song., Appl. Catal. B 98 (2010) 57–64.
[26] J.G. Seo, M.H. Youn, K.M. Cho, S. Park, S.H. Lee, J. Lee, K. Song., Kor. J. Chem. Eng. 25 (2008) 41–45.
[27] N.B. Klingoffer, F. Barrai, M.J. Castaldi, J. Power Sources 196 (2011) 6374–6381.
[28] B.D. Gould, X. Chen, J.W. Schwank, J. Catal. 250 (2007) 209–221.
[29] C.H. Bartholomew, Cat. Rev. Sci. Eng. 24 (1982) 67–112.
[30] D.L. Trimm, Catal. Today 37 (1997) 233–238.
[31] D.L. Trimm, Catal. Today 49 (1999) 3–10.
[32] X. Chen, B.D. Gould, J.W. Schwank, Appl. Catal. A 137–147 (2009) 356.
[33] J.P. Kopasz, D. Applegate, L. Miller, H.K. Liao, S. Ahmed, Int. J. Hydrogen Energy 30 (2005) 1243–1250.
[34] S. Yoon, I. Kang, J. Bae., Int. J. Hydrogen Energy 34 (2009) 1844–1851.
[35] S. Yoon, I. Kang, J. Bae., Int. J. Hydrogen Energy 33 (2008) 4780–4788.
[36] D.K. Liguras, D.I. Kondarides, X.E. Verykios, Appl. Catal. B 43 (2003) 345–354.
[37] J. Comas, F. Marino, M. Laborbe, N. Amandeo, Chem. Eng. J. 98 (2004) 61–68.
[38] J. Guo, H. Lou, X. Zheng, Carbon 45 (2007) 1314–1321.
[39] J. Park, J. Noh, J. Chang, S. Park., Catal. Lett. 65 (2000) 75–78.
[40] G.P. Ansell, S.E. Golunski, H.A. Hatcher, R.R. Rajaram, Catal. Lett. 11 (1991) 183–190.
[41] S.L. Lakhapatri, M.A. Abraham, Appl. Catal. A 364 (2009) 113–121.
[42] G. Garbarino, A. Lagazzo, P. Riani, G. Busca, Appl. Catal. B 129 (2013) 460–472.
[43] P.K. Cheekatamarla, W.J. Thomson, Appl. Catal. A 287 (2005) 176–182.
[44] P.K. Cheekatamarla, A.M. Lane., J. Power Sources 152 (2005) 256–263.
[45] K. Tomishige, T. Miyazawa, T. Kimura, K. Kunimori, N. Koizumi, M. Yamada, Appl. Catal. B 60 (2005) 299–307.
[46] A. Simson, Developing an Energy Efficient Steam Reforming Process to Produce Hydrogen from Sulfur-Containing Fuels (Ph.D. Thesis), Columbia University, New York, 2013.
[47] S. Cavallaro, V. Chiodo, S. Freni, N. Mondello, F. Frusteri, Appl. Catal. A 249 (2003) 119–128.
[48] M. Marquevich, S. Czernik, E. Chornet, D. Montane, Energy Fuels 13 (1999) 1160–11166.
[49] R. Coll, J. Salvado, X. Farriol, D. Montane, Fuel Process. Technol. 74 (2001) 19–31.
[50] E.C. Wanat, K. Venkataraman, L.D. Schmidt, Appl. Catal. A 276 (2004) 155–162.
[51] E.C. Vagia, A.A. Lemonidou, Int. J. Hydrogen Energy 32 (2007) 212–223.
[52] F. Tuinstra, J.L. Koening, J. Compos. Mater. 4 (1970) 492–499.
[53] A. Carrero, J.A. Calles, A.J. Vizcaino, Chem. Eng. J. 163 (2010) 395–402.
[54] L.F. Bobadilla, A. Alcarez, M.I. Dominguez, F. Romero-Sarria, M.A. Centeno, M. Montes, J.A. Odriozola, Appl. Catal. B 123–124 (2012) 379–390.
[55] A. Gallo, C. Pirovano, P. Ferrini, M. Marelli, R. Psaro, S. Santangelo, G. Faggio, V.D. Santo, Appl. Catal. B 121–122 (2012) 40–49.
[56] J.M. Chalmers, P.R. Griffiths (Eds.), Handbook of Vibration Spectroscopy-Sample Characterization and Spectral Data Processing, vol. 3, John Wiley & Sons, Inc., Chichester, 2002, pp. 1846.
[57] A.R. Greenwood, K.D. Vesely, Inventors; Universal Oil Products Company, assignee. Continuous Reforming-regeneration Process. US patent 3,647, 680.
[58] T. Giroux, E. Waterman, R. J. Farrauto, inventors; BASF Corporation, Assignee. Reforming Sulfur-containing Hydrocarbons Using a Sulfur Resistant Catalyst. US patent 7,901,565 B2 (2011).
[59] X. Liu, W. Ruettinger, X. Xu, R. Farrauto, Appl. Catal. B 56 (2005) 69–75.
[60] M.G. Poirier, C. Sapundzhiev, Int. J. Hydrogen Energy 22 (1997) 429–433.
[61] A. Simson, R. Farrauto, M. Castaldi, Appl. Catal. B 106 (2011) 295–303.